



Energy-absorbing limitations of hard hat safety helmets in mitigating trauma from falling objects

Mariusz Ptak¹ · Mateusz Dymek¹ · Daniel Wdowicz^{1,2} · Adrianna Szumiejko¹ · Artur Kwiatkowski^{3,4}

Received: 15 April 2024 / Revised: 7 June 2024 / Accepted: 30 June 2024
© The Author(s) 2024

Abstract

The aim of the study was to analyze the effectiveness of hard hat helmets in mitigating head injuries from high-energy falling objects through a real-world case study, advanced numerical simulations and an uncertainty study. The study aims to answer the following research questions: (a) to what extent would the use of the protective helmet limit the kinetic energy of the falling construction prop, (b) whether the hard hat helmet would be damaged, and if so, to what extent, according to the helmet standards? A fatal construction accident involving a falling prop impact on the victim's head was reconstructed using multi-body dynamics simulations and finite element analysis (FEA) based on uncertainty-based determination of initial conditions. The study quantified the impact energy, helmet damage and its energy-absorbing capabilities, and potential injury reduction compared to scenarios without a helmet. While the helmet absorbed significant energy (245% of the standard requirement) and reduced the Head Injury Criterion by 8–11%, the high impact energy ultimately proved fatal. This study highlights the limitations of hard hat helmets in extreme scenarios with high kinetic energy impacts. While helmets offer valuable protection, unrealistic expectations should not be placed on their ability to prevent all head injuries. The study not only enhances our understanding of the biomechanics of head injuries in such incidents but also provides practical implications for safety protocols and regulations.

Keywords Head injury · Construction site · Helmet · Hard hat · Safety · Multi-body · Finite element method

1 Introduction

According to estimates by Takala [1], approximately 335,000 fatalities resulted from occupational injuries globally. In the European Union (EU), Eurostat data reveal fatal occupational injury rate to be 6.1 per 100,000 employed individuals in 1994 and 4.8 in 1999 for the entire EU region [2]. According to Personick [3], machinery, building materials,

and vehicles account for nearly 40 percent of the primary objects cited when workers are fatally struck in a workplace. That includes various falling, flying, swinging, and rolling objects such as cranes and other material handling machinery, metal pipes, steel beams, dimensional lumber, trucks, and tractors. Aneziris [4] classified five groups of people with a high risk of being hit by a falling object. They are people working: (1) with or near cranes, (2) near mechanical lifting equipment other than cranes, (3) with or near person-propelled vehicles, (4) near manual handling of loads or (5) near falling objects.

Hard hat helmets, also known as safety helmets or construction helmets, are a crucial piece of personal protective equipment (PPE) [5] designed to protect a user's head from impact, falling objects, and electrical hazards in various industrial and construction facilities [6–8]. Helmets serve not only to protect the skull from puncture but also to reduce the impact force transferred to the wearer from the object of collision [8]. The helmets are constructed with a hard outer shell usually made from high-density polyethylene or polycarbonate [9], which is designed to distribute the impact

✉ Mariusz Ptak
mariusz.ptak@pwr.edu.pl

¹ Faculty of Mechanical Engineering, Wrocław University of Science and Technology, Łukasiewicza, 7/9, 50-371 Wrocław, Poland

² CYBID Sp. Z O.O. Sp. K., Ul. Kuźnicy Kołłątajowskiej, 31-234, 15C/L2 Kraków, Poland

³ Department of Neurosurgery, Provincial Specialist Hospital in Legnica, Iwazkiewicza, 5, 59-220 Legnica, Poland

⁴ Faculty of Medicine, Wrocław University of Science and Technology, Hoene-Wrońskiego 13c, 58-376 Wrocław, Poland

force over a larger area, thus preventing penetration. Moreover, the curved surface of a helmet enables more predictable deflection of impact, potentially causing rotational forces on the head [10, 11]. Interestingly, hard hat helmets do not typically include shock-absorbing foam. The helmets are primarily comprise a hard outer shell designed to provide protection against penetration and blunt impact. The absence of polymeric foams, which notably are used in other types of helmets for impact absorption, can be attributed to the specific design requirements and intended use of hard hat helmets. However, inside the shell, a suspension system is incorporated to provide a comfortable and secure fit while absorbing an impact kinetic energy. The suspension system (the frame) helps distribute the force of an impact, mitigating the effect of the impact on the wearer's head.

In addition, many hard hats are equipped with accessories such as face shields, earmuffs, and chin straps to provide additional protection and stability for a user. The use of hard hats is mandated by safety regulations in many industries to mitigate the risk of head injuries and ensure the safety of workers in hazardous environments such as construction and mining [12]. Long [8] and Jacob [13] contributed to the development of biomechanical finite element (FE) models for the human head, with a focus on the effectiveness of construction safety helmets. Long [8] specifically developed an FE model to study the effectiveness of these helmets, while Jacob [13] used their model to simulate and predict the responses of safety helmets under varying impact heights. Wu [14] built on this work by modifying the FE models to assess the effect of neck and body mass during impact on a construction safety helmet and relative responses on a head-brain model. These studies collectively highlight the importance of FE models in predicting the forces or energy transferred to the head during an impact, as well as how the importance of the construction of the helmets.

For years, scientists and researchers have been working on improving how accidents are reconstructed. To understand what happens during accidents, they use different methods. Multi-body (MB) dynamics simulations are one way they accomplish this. The concept of MB modeling involves representing mechanical systems as chains of interconnected rigid bodies, linked by kinetic pairs or joints, to simulate motion. This motion is calculated using the Newton–Euler equations [15]. By MB modeling, scientists can recreate the movement of objects and people involved in accidents. This approach gives researchers a better and more complete understanding of the mechanical parameters, such as forces and accelerations involved in these events. A range of studies have contributed to the advancement of accident reconstruction through multi-body dynamics simulations. Olson [16] proposed a modular approach, using interactive numerical modules to reconstruct the physical events of an accident. Shen [17] improved the numerical reconstruction

of vehicle–pedestrian accidents by introducing a sequential linear programming method and a new anthropometry model. Portal and Dias [18] developed methodologies for road accident reconstruction using 3D multi-body rigid dynamics, including contact-impact models and plastic elements. Steffan [19] focused on simulating multiple vehicles' pre-collision, collision, and post-collision dynamics, introducing trajectory and collision models and optimization strategies. Collectively, these studies demonstrate the significant progress made in accident reconstruction through MB dynamics simulations. Researchers have employed simplified MB models to reconstruct accidents involving complex dynamics [18–22]. Furthermore, MB modeling has been utilized mostly in the reconstruction of vehicle–pedestrian accidents but demonstrates its applicability to various scenarios [17, 18, 23–27].

The novelty of this study lies in its comprehensive integration of MB dynamics and finite element analysis (FEA) to investigate the effectiveness of safety helmets in mitigating head injuries from falling objects, specifically focusing on high-energy incidents. Unlike previous studies that primarily focused on low-impact scenarios or simplified models, our approach provides a detailed reconstruction of the incident also incorporating uncertainty analysis. This research not only enhances our understanding of the protective capabilities of safety helmets, but also offers practical insights into improving safety protocols and regulatory standards in high-risk environments.

The case study performed in this paper is based on a fatal accident at work caused by a falling construction prop on a man's head. A series of simulations were conducted to evaluate the potential mitigating effects of hard hats in high-energy incidents. The study not only enhances our understanding of the biomechanics of head injuries in such incidents but also provides practical implications for safety protocols and regulations.

2 Materials and methods

The method of accident analysis presented in this paper is depicted in Fig. 1. This comprehensive methodology integrates computational tools, simulations, physical testing, and analytical techniques to provide a robust and detailed analysis of the accident scenario, ensuring a thorough understanding of the incident and its contributing factors. This stepwise approach facilitates a systematic investigation, allowing for accurate reconstruction and analysis of the events leading to the described accident.

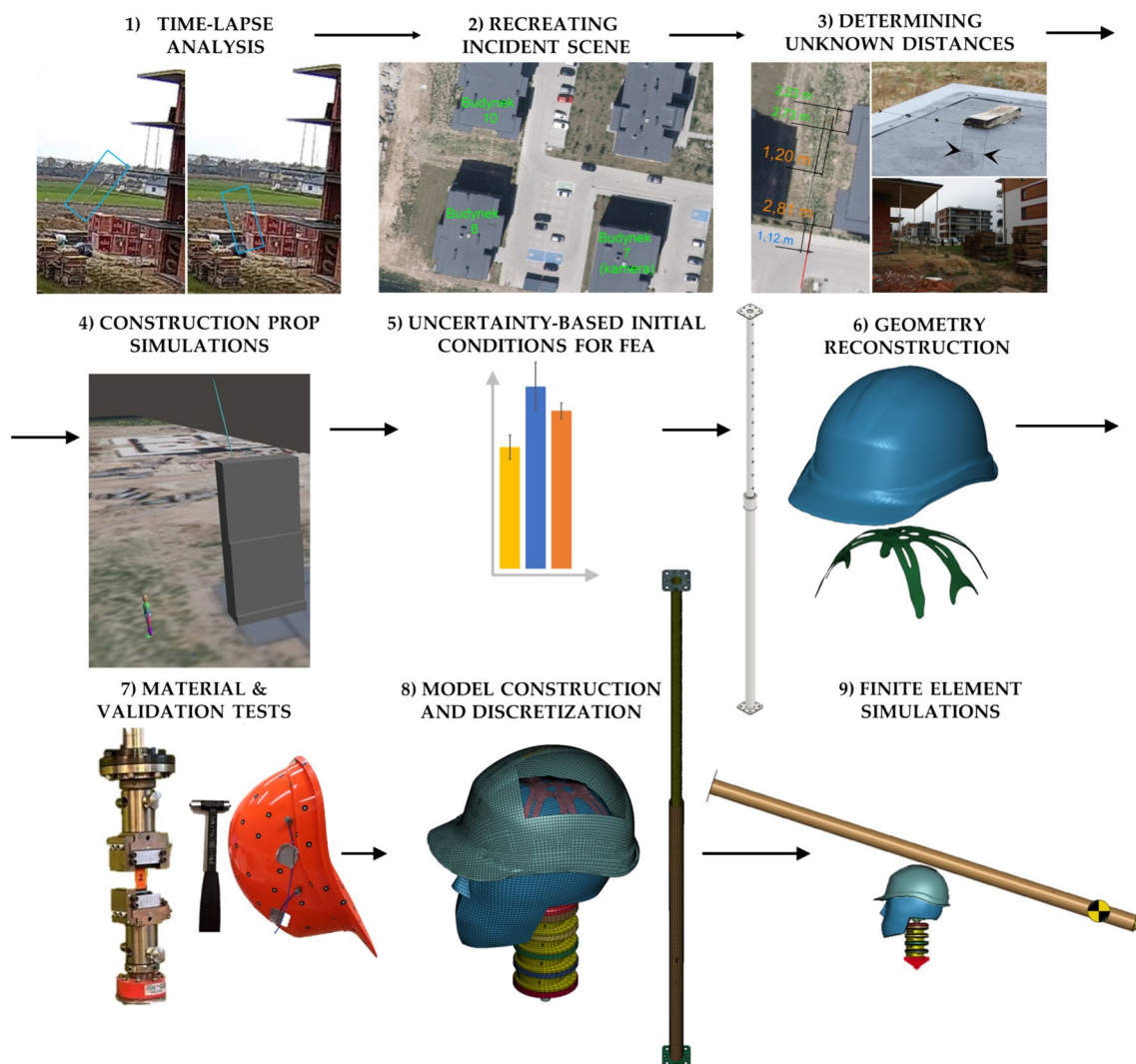


Fig. 1 Flowchart of the used approach for the accident analysis

1. Development of Python script for time-lapse analysis: Developing a Python script to perform time-lapse analysis, aiding in the systematic examination of the incident.
2. Recreation of incident scene: Recreating the incident scene using V-SIM 5.0, incorporating photos and ortho-photo maps to generate a virtual representation.
3. Determination of unknown distances: Determining unknown distances within the incident scene by referencing case file photos and utilizing objects of known length as reference points.
4. Simulations of construction prop fall: Conducting simulations to model and analyze the fall of the construction prop within the virtual environment of V-SIM 5.0.
5. Uncertainty-based determination of initial conditions for FEA: Establishing initial conditions for the subsequent FEA based on the outcomes of the simulations.
6. Reconstruction of geometry: Reconstructing the geometry of the construction prop and the protective helmet involved in the incident to provide accurate representations for further analysis.
7. Physical material and validation tests: Conducting physical material tests to gather data on the mechanical properties of the materials, ensuring realistic and reliable input for subsequent simulations. Further, the full-scale model validation, based on dynamic modal analysis, was carried out.
8. Discretization and assignment of material data: Discretizing the protective helmet and construction prop models, breaking them down into finite elements, and

assigning appropriate material data based on the results of the physical material tests.

- Finite element simulations in LS-DYNA: Performing FEA simulations using the discretized models and assigned material data to analyze the structural behavior and response of the hard hat and construction prop under various conditions.

2.1 Accident reconstruction

The analyzed accident occurred at a construction site. A 13.1-kg construction prop, which had been mounted as support between two balconies (Fig. 2a), slipped from its deployed position on the second-floor balcony and hit an employee who was at that time at his break at the ground (zero) level. As stated in the case files, the employee was a crane operator, and he was not a part of the regular construction crew who mounted the prop. At the time of the accident, he was not wearing a helmet.

The medical autopsy reported multiple injuries sustained by the victim: skull fractures with intussusception of bone fragments into the skull cavity, skull base bone fractures and brain trauma, brain contusions in the brain stem and cerebellum, hemorrhages in the mastoid cavities, bleeding in the basal part of the brain, and a coexisting spine fracture.

To model the prop-to-head impact, initial conditions of the impact, i.e., kinematics of the prop at the moment of contact with the employee's head, had to be determined. However, the case files yielded little useful information in this regard. Photographic documentation was sparse, and there were no detailed testimonies. The construction had been finished multiple years before the reconstruction, with

the building's yard rearranged, and no relevant measurements could be taken on-site.

A single recording from a closed-circuit television (CCTV) camera was available, and in the initial stage of the accident reconstruction process, a time-lapse analysis was attempted. Dedicated Python programming languages were developed for this purpose. However, low quality and framerate of the recording prevented the velocity of the prop in-flight from being reliably established, and due to the camera's point of view, the victim's location was obscured by a set of wooden pallets (Fig. 2b). In the end, it was decided to use a preliminary multi-body simulation to determine the kinematics of the prop.

CYBID V-SIM 5.0 software was chosen for this purpose. It is a reconstruction software package equipped with multiple functionalities for integration of criminal evidence (photographs, point-cloud measurements, spatial data from online databases), recreating the accident environment in 3D, and then using the created environment for a simulation of vehicle dynamics or multi-body simulation of human body dynamics [15].

As an input for the multi-body simulation, three geometric measurements had to be determined: horizontal distance from the victim to the side of the building, height of the balcony in relation to the ground level, and distance between the base of the prop and the edge of the balcony.

As no specific information was available in the case files, these measurements were approximated using the available photographs taken after the accident and the accident sites' spatial data, which was imported into the simulation environment using built-in functionalities of V-SIM.

Due to the inherent uncertainty of the approximations, the uncertainty approach was used. This approach is commonly recommended for purposes of vehicular accident reconstruction [28, 29]. Each of the three approximated values was analyzed within the uncertainty range, which range was discretized using an iteration step. The approximated values, uncertainty range, and iteration step are presented in Table 1.

For the purposes of multi-body simulation, the prop was modeled as a cylinder, and it was slightly rotated in relation to ground level to allow for a gravitational fall of it onto the human body model (Fig. 3). The human body model was 1.75 m tall, which was the stature of the victim reported in the files. The model was created using a V-SIM-integral human body generator, which generates a set of anthropometric dimensions based on combined data from American–German and Polish specimens [15].

The process of setting up and running simulations was automatized using V-SIM API scripting interface and scripts written in Lua programming language. Using the API, each simulation was automatically stopped whenever the impact of the prop to the head was detected, and the position and velocity of the prop in relation to the head were reported. The contact detection was performed using an inherent

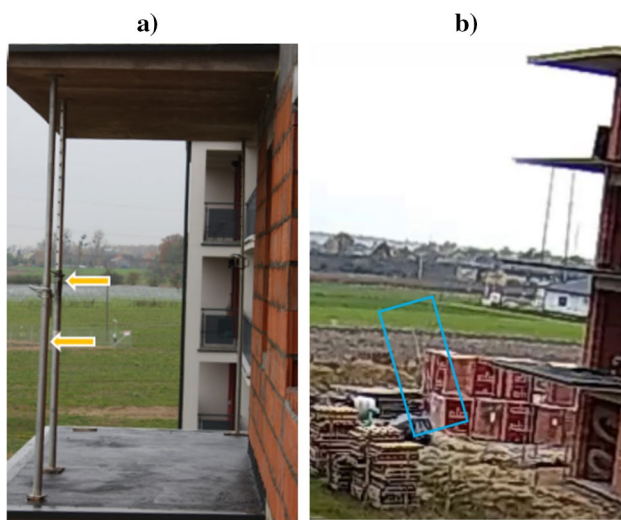


Fig. 2 **a** General view of deployed construction props (indicated by arrows); **b** sample frame from the CCTV recording. As the prop is blending in the background, its position is marked with a blue rectangle. The victim is obscured by wooden pallets

Table 1 Uncertainty matrix

Size	Approximated value	Range of values considered based on uncertainty range	The adopted iteration step of a given quantity	Number of configurations
Horizontal distance from the victim to the side of the building	2.23 m	1.83 m – 2.63 m	0.10 m	9
Height of the balcony in relation to the ground level	6.90 m	6.40 m – 7.40 m	0.20 m	6
Distance between the base of the prop and the edge of balcony	0.42 m	0.30 m – 0.54 m	0.04 m	7
			Total	$9 \cdot 6 \cdot 7 = 378$

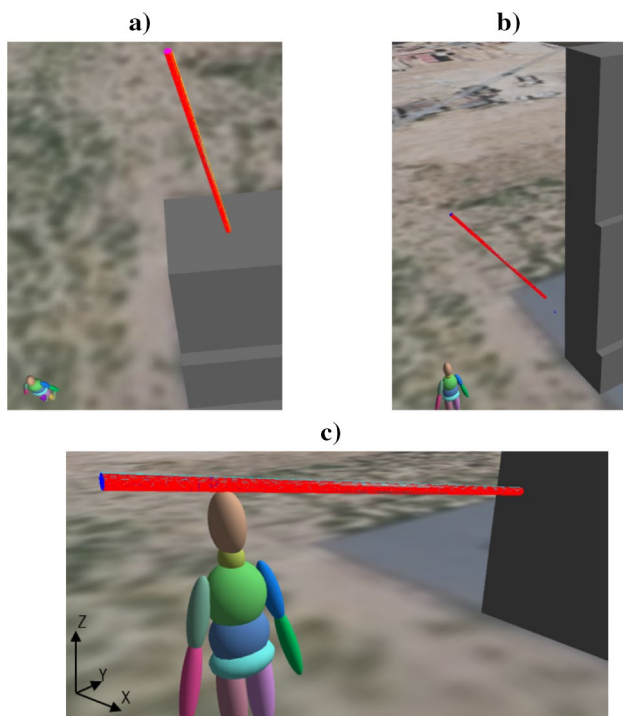


Fig. 3 Simulation stages' footages from multi-body software V-SIM: **a** starting moment of the simulation of the fall of the construction prop (for the selected geometry configuration of the incident site); **b** construction prop in-flight; **c** the moment of impact of the construction prop to the head of the human body model

volumetric contact model. The model worked by discretizing the volumes of the objects involved, such as the prop and the

head, into small cubes called voxels. Contact was detected when these voxels intersect. After completing a simulation, the V-SIM API was able to determine the exact time of the first contact. This timing information was crucial for analyzing the kinematics at the moment of contact. Using this specific time, we were able to extract a detailed simulation log that includes the linear and angular velocities and positions of the prop, enabling a comprehensive analysis of the kinematics involved in the contact event.

In total, 378 multi-body simulations were run. In each of the simulations, the prop first impacted the head of the victim, and then it impacted the ground. The kinematics of the prop was corroborated by the CCTV recording. The summary of the 378 simulations is presented in Table 2. For the FE simulations, it was decided that the average value of each kinematic parameter would be used.

2.2 Numerical modeling and experimental validation

To carry out the numerical simulations of the construction prop impact on the victim's head, it was necessary to reproduce the geometry of the building punch in accordance with the technical documentation, build a discrete model, and conduct a simulation with the Hybrid III head and neck model (Fig. 4). The construction helmet was scanned with a ZEISS T-SCAN Hawk 2 scanner. Based on the 3D scan, the initial geometry of all helmet components was obtained and discretized. The missing harness was modeled to the helmet with a *Seatbelt* element in LS-DYNA explicit code [30].

Table 2 Average and standard deviation of kinematic parameters of the construction prop at the moment of impact to the head ($N=378$ multi-body simulations)

	Arithmetic average	Standard deviation
The value of the angle of inclination of the construction prop relative to the vertical axis	71.97°	9.25°
Linear velocity of the center of gravity of the construction prop: X component	- 1.48 m/s	0.04 m/s
Linear velocity of the center of gravity of the construction prop: Z component	- 10.91 m/s	0.27 m/s
Angular velocity of the construction prop: Y component	3.88 rad/s	0.17 rad/s

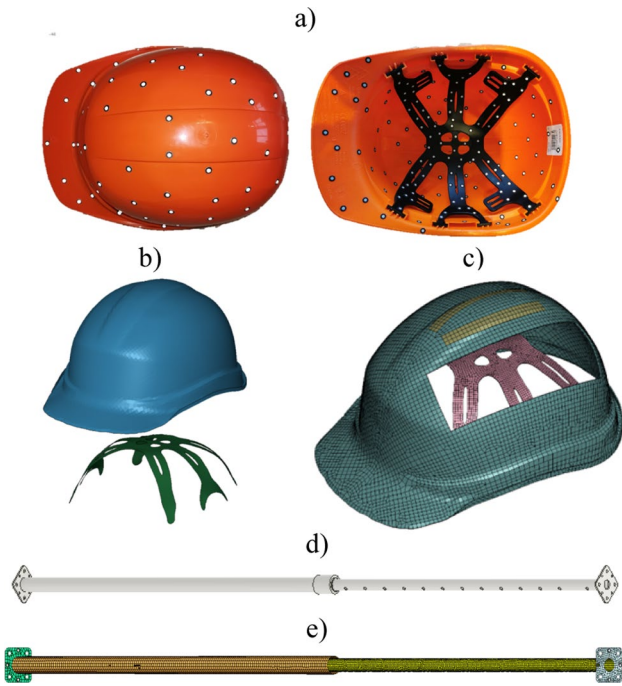


Fig. 4 The used hard hat helmet (top): **a** physical helmet prepared for 3D scanning **(b)** CAD and **(c)** FE model and the construction prop (bottom): **d** CAD and **e** FE model

A Zwick/Roell testing machine was used to develop the material parameters of the helmet components. A series of samples of the helmet shell and harness were prepared for the tensile test. A visualization of one of the tests and a summary of the parameters are shown in Table 3. The material model for the shell and for the suspension system (frame) that included mechanical parameters is depicted in Table 3, along with individual stress–strain curves with damage function. The material was indicated by the helmet’s


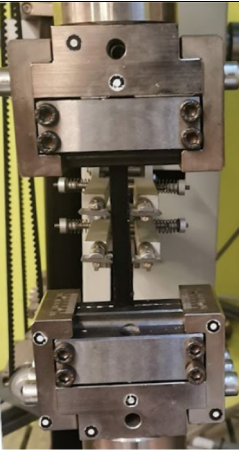
manufacture. The construction prop was assigned the material data of steel (density [kg/m³] 7 830; Young’s modulus [GPa] 210; Poisson’s ratio 0.3) without plasticity, as the mechanical properties are significantly stiffer than the human head.

The hard hat helmet model validation, through dynamic modal analysis, is depicted in Fig. 5. The experimental validation (stage 1) of the helmet’s dynamic response involved instrumenting the helmet with accelerometers and designing a test setup to replicate the FE environment (so-called free boundary conditions) as accurately as possible. A testing protocol was developed for controlled impact loading, and dynamic response testing was conducted accordingly. The FE code post-processor determined the modal hammer accelerometer locations. The helmet was suspended on a thin rope to reflect free boundary conditions in FE. Sensors were fixed to the sides of the helmet, with impacts applied to the opposite side. Experiments were conducted using various modal hammer tip stiffnesses and masses.

During testing, data on acceleration were collected, and subsequent analysis was performed to assess the helmet’s dynamic behavior [31, 32]. Output analysis, in terms of acceleration, included Fourier spectrum analysis to verify frequencies. This analysis included evaluating resonant frequencies, and deformation patterns. Further (stage 2), experimental results were compared with simulations carried out in Abaqus CAE. The analysis indicated very good agreement for physical helmet and its numerical model at frequencies of 250 Hz.

The numerical modal analysis (stage 2) results for a hard hat helmet simulated in Abaqus CAE included information about the natural frequencies and mode shapes of the helmet structure. The same material model, specifically the piecewise linear plastic model, was utilized in both numerical codes, LS-DYNA and Abaqus CAE. These models were parameterized using the same mechanical properties

Table 3 Visualization of sample tests and summary of material parameters of the hard hat

Tensile tests		Hard hat mechanical parameters			
		Component	Material	Young’s modulus [GPa]	Yield strength [GPa]
		Shell	High-density polyethylene (HDPE)	1.240	0.01993
		Suspension system (Frame)	Low-density polyethylene (LDPE)	0.225	0.00775

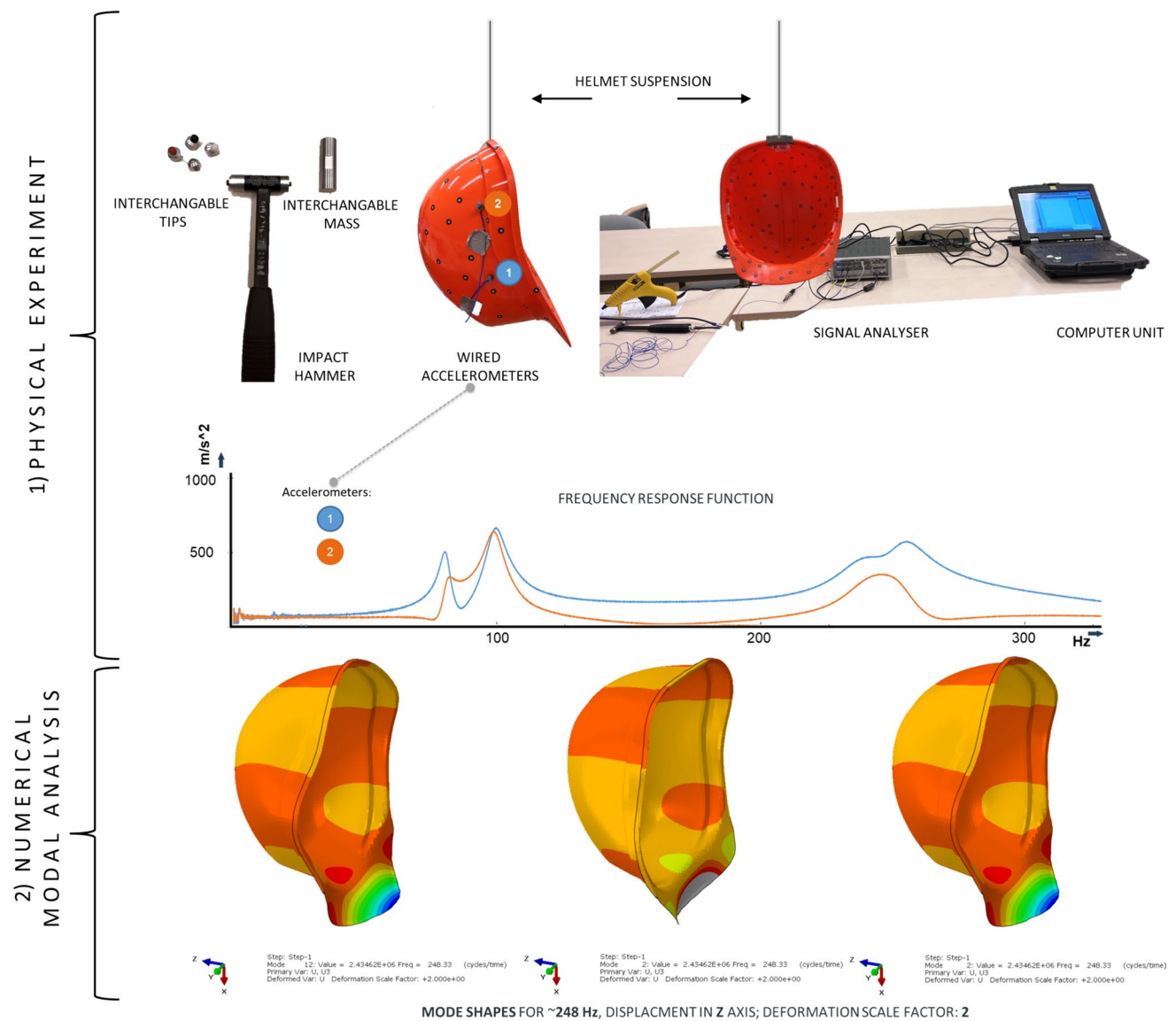


Fig. 5 Hard hat helmet model validation approaches in two stages: (1) physical and (2) numerical (mode shapes for circa 248 Hz, displacement in Z axis, deformation scale factor: 2)

obtained from experimental tests. By maintaining consistency in the material model, Abaqus CAE provided a list of natural frequencies along with their corresponding mode numbers and frequencies. Abaqus CAE displayed graphical representations of mode shapes for each mode, showing the displacement or deformation patterns of the helmet structure. The listed modes agreed well for both physical and numerical approaches except for the initial rigid body modes registered in Abaqus CAE for the values < 1 Hz.

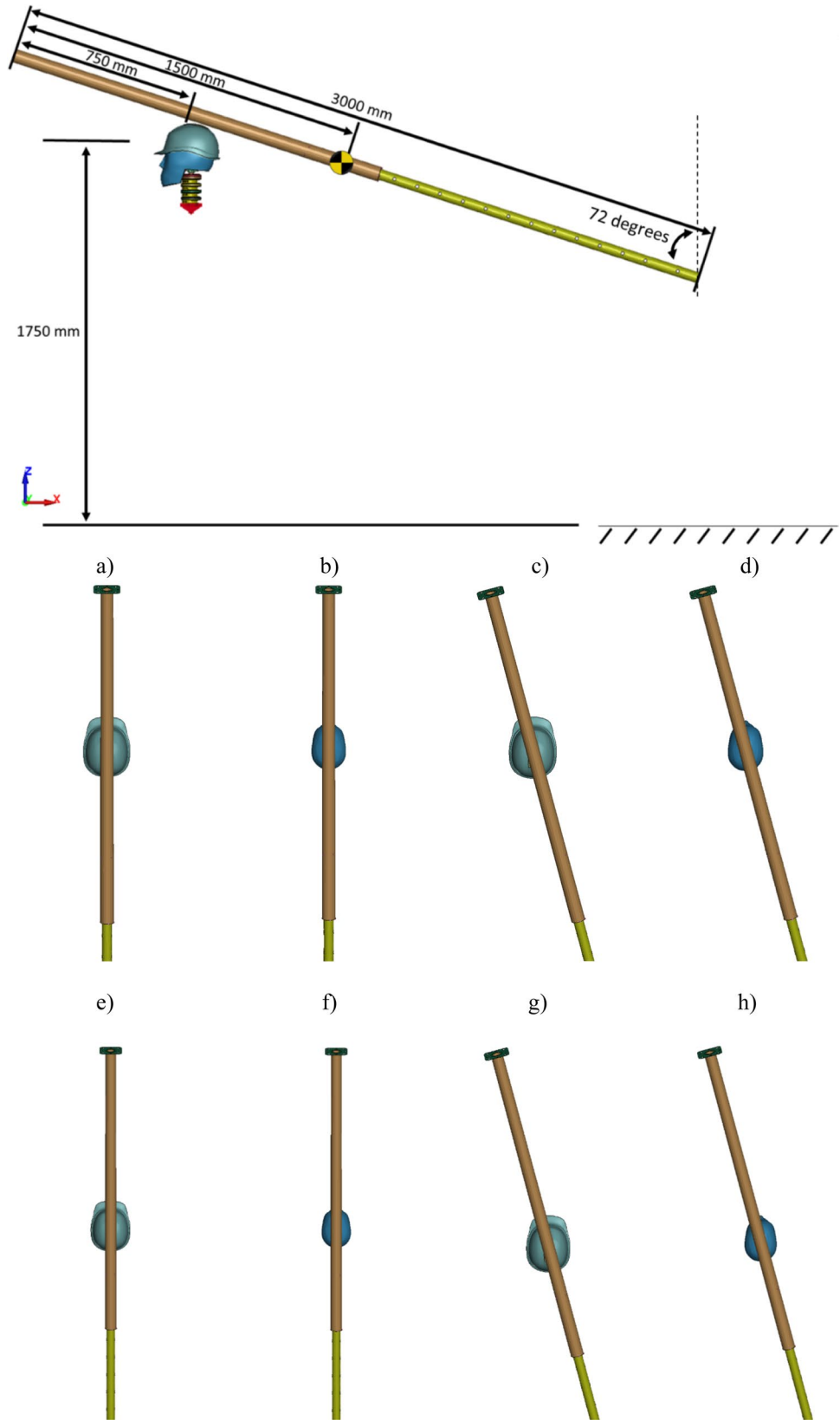
2.3 Simulation configuration matrix

The simulation preparation consisted of positioning the Hybrid III head model at a height corresponding to the

Injured Person in accordance with the data from the files: 1.75 m. The construction helmet was positioned on the head model using a force in accordance with the PN-EN 397 + A1 standard: 50 N acting along the vertical axis.

According to the accident files, the skull fracture was located in the occipital region of the head. Based on that information and the multi-body simulation results, it was assumed that the point of contact was in the occipital head region. To assess the injury, it was decided to conduct the following configuration matrix that is summarized below and in Fig. 6, where (a), (c), (e), (g) are simulations of Hybrid III equipped with a helmet and (b), (d), (f), (h) are simulations of Hybrid III only. The impact configurations are as follows:

Fig. 6 Visualization of one of the numerical simulations with the given dimensions and center of mass of the construction prop; each configuration representation from top view: a, c, e, g—Hybrid III with hard hat; b, d, f, h—Hybrid III



The back of the head equipped with a construction hard hat with a construction prop, halfway along the outer prop—(a)

The back of the head with a construction prop, halfway along the outer prop—(b)

The back of the head equipped with a construction hard hat with a construction prop rotated by 15°, halfway along the outer prop—(c)

The back of the head with a construction prop rotated 15°, halfway along the outer prop—(d)

The back of the head equipped with a construction hard hat with a construction prop, in one-third of the length of the outer tube, counting from the center of gravity of the entire prop—(e)

The back of the head with a construction prop, in one-third of the length of the outer prop, counting from the center of gravity of the entire prop—(f)

The back of the head equipped with a construction hard hat with a construction prop rotated by 15°, in one-third of the length of the outer prop, counting from the center of gravity of the entire prop—(g)

The back of the head with a construction prop rotated by 15°, in one-third of the length of the outer prop, counting from the center of gravity of the entire prop—(h)

In the considered time interval (approximately 4 ms before the contact of the construction prop with the hard hat and approximately 10 ms after contact), the bottom of the numerical model of the neck was fixed in space. This boundary condition will allow the collection of reliable data with respect to the observed human body behavior in real-life cases [33].

2.4 Assessment of the kinetic energy and energy absorption

In this chapter, we present the assessment of the kinetic energy of the construction prop and the energy absorbed by the hard hat in accordance with the PN-EN 397 + A1 standard. Based on the multi-body simulation results and CAD data, the following parameters of the construction prop were determined (Table 4):

Table 4 Physical parameters of the impacting construction prop

The value of the angle of inclination of the construction prop relative to the vertical axis	$\alpha = 71.97\text{deg}$
Linear speed, X component	$V_{linx} = 1.48\text{m/s}$
Linear speed, Z component	$V_{liny} = 10.91\text{m/s}$
Construction prop angular velocity, Y component	$\omega = 3.88\text{rad/s}$
PEP ALPHA-2 B-300 prop mass	$m = 13.10\text{kg}$
Moment of inertia around the Y axis of the center of mass of the prop	$I = 9622265.114\text{kg} \cdot \text{mm}^2 \approx 9.6223\text{kg} \cdot \text{m}^2$

The linear speed of the construction prop was determined from the vector addition formulas:

$$V_{lin} = \sqrt{V_{linx}^2 + V_{liny}^2} = \sqrt{1.48^2 + 10.91^2} \approx 11.01 \text{ m/s} \tag{1}$$

Then the linear and angular kinetic energies were calculated:

$$\begin{aligned} \text{Linear kinetic energy } E_{klin} &= \frac{m \cdot V_{lin}^2}{2} \\ &= \frac{13.10\text{kg} \cdot (11 \text{ m/s})^2}{2} \approx 792.55 \text{ J} \end{aligned} \tag{2}$$

$$\begin{aligned} \text{Angular kinetic energy } E_{kkat} &= \frac{I \cdot \omega^2}{2} \\ &= \frac{9.62\text{kg} \cdot \text{m}^2 \cdot (3.88 \text{ rad/s})^2}{2} \approx 72.43 \text{ J} \end{aligned} \tag{3}$$

$$\begin{aligned} \text{Total kinetic energy } E_k &= E_{klin} + E_{kkat} \\ &= 792.55 \text{ J} + 72.43 \text{ J} = 864.98 \text{ J} \end{aligned} \tag{4}$$

Numerical simulations show that the construction prop’s kinetic energy at the moment of impact is consistent with analytical calculations. The kinetic energy of the construction prop at the moment of impact is approximately 865 J. The authors, using numerical simulations, determined that the construction hard hat absorbed 120 J (value calculated on the basis of the arithmetic mean of four simulations; the individual components are 140 J, 110 J, 120 J, and 110 J). Compared to the PN-EN 397 + A1 standard, point 6.6.3, the hard hat absorbed 245% of the energy required by the standard (mass of the impactor: 5 kg; height of the impactor above the hard hat: 1 m; calculated energy: 49 J).

3 Results and discussion

Accident reconstruction is a multidisciplinary field that plays a crucial role in understanding and analyzing the dynamics of events, providing valuable insight into not only the actions

leading to an accident but also the circumstances of the accidents. In recent years, the integration of advanced simulation techniques has significantly enhanced the accuracy and comprehensiveness of accident reconstructions.

The Head Injury Criterion (HIC) index is crucial in assessing head injury risk. It is calculated as the maximal integral value from the linear acceleration function within time boundaries of 36 ms. The study found that for each variant of a hard hat collision, the HIC index value was above 7 800. According to the state of knowledge in the field of biomechanics of collisions, a value of the HIC index exceeding 3 000 indicates a situation with a very high probability of fatal injuries [34–37].

The results of numerical simulations showed a reduced value of the HIC parameter by 8% for configurations (a) and (b), 11% for configurations (c) and (d), 10% for configurations (e), (f), (g), and (h). The acceleration curves of the head center of mass and the visualization of the HIC parameter are included in Appendix No. 1, and a summary of the HIC is presented in Table 5.

Based on the reconstruction of the accident (in particular, by determining the speed of the construction prop at

the moment of impact), it was estimated that the kinetic energy of the construction prop at the moment of impact was approximately 865 J. It was found that the energy transferred in presented impacts to the Hybrid III head model (without a hard hat) led to very high head acceleration values. The HIC values for simulations without a hard hat reached over 8 700. It was calculated that a construction hard hat would absorb approximately 120 J of energy under the same impact conditions. The use of a hard hat reduced HIC by approximately 8–11%. Figure 7 presents a visualization of the impact with a construction hard hat. The time step presented is 3 ms.

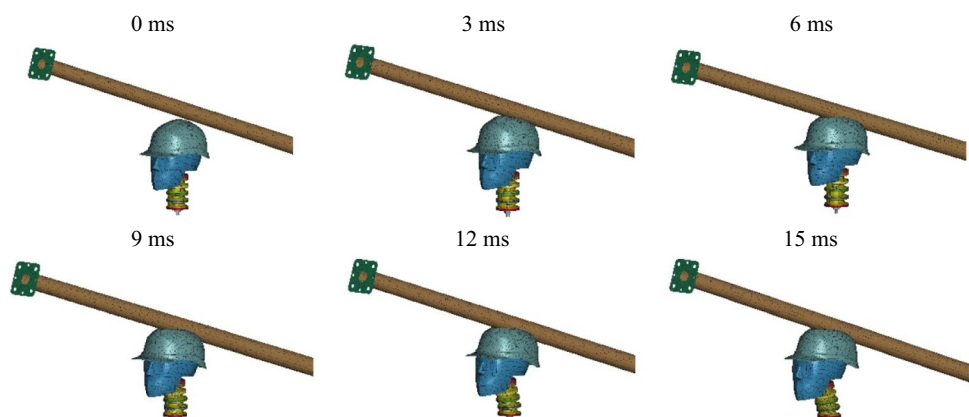
Accident reconstruction, especially in the context of evaluating the energy of a falling object and the effectiveness of protective gear, has been the subject of significant research [38–41]. The described accident is identified through detailed incident reports, eyewitness accounts, and a complex forensic reconstruction involving various numerical approaches such as FEA and multi-variant multi-body simulations.

The accident reconstruction was made based on a case study. It aimed to determine the energy of the construction prop falling from the balcony onto the victim's head during

Table 5 Simulation setup and HIC values

No	Summary of HIC values for the simulation	
a)	An impact to the back of the head equipped with a construction hard hat with a construction prop, halfway along the outer prop	9 502
b)	An impact to the back of the head with a construction prop halfway down the outer prop	10 370
c)	An impact to the back of the head equipped with a construction hard hat with a construction prop rotated 15° halfway along the outer prop	7 810
d)	An impact to the back of the head with a construction prop rotated 15° halfway along the outer prop	8 774
e)	An impact to the back of the head equipped with a construction hard hat with a construction prop, in one-third of the length of the outer tube, counting from the center of gravity of the entire prop	8 354
f)	An impact to the back of the head with a construction prop, in one-third of the length of the outer prop, counting from the center of gravity of the entire prop	9 273
g)	An impact to the back of the head equipped with a construction hard hat with a construction prop rotated by 15°, in one-third of the length of the outer prop, counting from the center of gravity of the entire prop	8 250
h)	An impact to the back of the head with a construction prop rotated by 15°, in one-third of the length of the outer prop, counting from the center of gravity of the entire prop	9 229

Fig. 7 Configuration (a) time step visualization: a blow to the back of the head equipped with a construction hard hat with a construction prop, halfway along the outer prop



the incident as well as to what extent the use of the protective hard hat assigned to him would limit this energy, whether the hard hat would be damaged, and if so, to what extent in relation to the protection standards met by the hard hat that the victim was supposed to use. This was accomplished by a multi-body-based accident reconstruction with elements of an uncertainty study and a finite element simulation using validated models.

The use of hard hats in accident situations has been studied through advanced numerical simulations, leading to the conclusion that these hard hats can reduce the overloads acting on the head. The authors found that under similar collision conditions, a construction hard hat would absorb approximately 120 J of energy, reducing the Head Injury Criterion (HIC) index value by approximately 8–11%. Furthermore, the study compared the energy absorption capacity of the hard hat to the PN-EN 397 + A1 standard and found that the hard hat would absorb 245% of the energy required by the standard, indicating that it would likely be damaged in such situations [42]. The use of hard hats in reducing head injury risk has been a subject of interest in various fields. The advanced numerical simulations conducted by the authors provide valuable insights into the effectiveness of construction hard hats in reducing head injury risk [43]. The findings underscore the importance of hard hats in mitigating the overloads acting on the head during accidents, as evidenced by the significant energy absorption and reduction in HIC index values. However, the study also emphasizes the need for further research to enhance understanding of the role protective gears for reducing head injuries.

4 Conclusion

In this study, we focus on evaluating the effectiveness of hard hats in mitigating trauma from falling objects, particularly in high-energy incidents. Through advanced biomechanical analyses and multi-body dynamics simulations, we investigate the limitations of these hard hats in extreme scenarios where the kinetic energy involved can be fatal despite protective measures.

Based on previous research on hard hats and accident reconstruction methodologies, we present a case study involving a fatal workplace incident caused by a falling construction prop. Our aim is to quantify the energy of the falling object and assess the extent to which the assigned protective hard hat limits this energy, considering both potential damage to the hard hat and its effectiveness in reducing head injury severity.

Our findings reveal that while construction hard hats can absorb a significant amount of energy and reduce head injury criteria indices by approximately 8–11%, they may still be inadequate in extreme situations. Comparison with industry standards indicates that hard hats may absorb more energy than required by regulations, suggesting potential damage during high-energy impacts.

Overall, this research underscores the importance of considering the limitations of hard hats in high-energy incidents and emphasizes the need for comprehensive risk mitigation strategies in occupational settings where falling objects pose a significant hazard. The ultimate idea of the presented research was to address the questions stated by the authorities:

To what extent would the use of the protective hard hat limit the energy, whether it would be damaged, and if so, to what extent, according to the construction hard hat standards?

Based on the results of numerical simulations, it was concluded that the use of a hard hat in such accidents would slightly reduce the accelerations acting on the head center of mass. As the literature in the biomechanics field indicates, such HIC values (exceeding 3 000) indicate a situation with a very high probability of fatal injury.

Compared to the PN-EN 397 + A1 standard, the hard hat would absorb 245% of the energy required by the standard, which is well above the set limit. Thus, it would be highly probable that the hard hat would be penetrated and there would be direct contact between the construction prop and head. It should be highlighted that the presented impacts are defined with the construction prop falling from approximately 6.9 m, which leads to high impact velocity. In this specific scenario, the hard hat would slightly minimize HIC and, thus, injury probability.

The study contributes to the understanding of hard hat effectiveness in mitigating head injuries and underscores the need for continuous improvement in protective gear design and workplace safety protocols. Despite some limited effectiveness for high-impact energies, the authors strongly suggest wearing the protective equipment at all times necessary and taking all possible precautions.

Appendix

1. Graphs showing the resultant accelerations of the center of mass of the head model

See Figs. 8, 9, 10, 11.

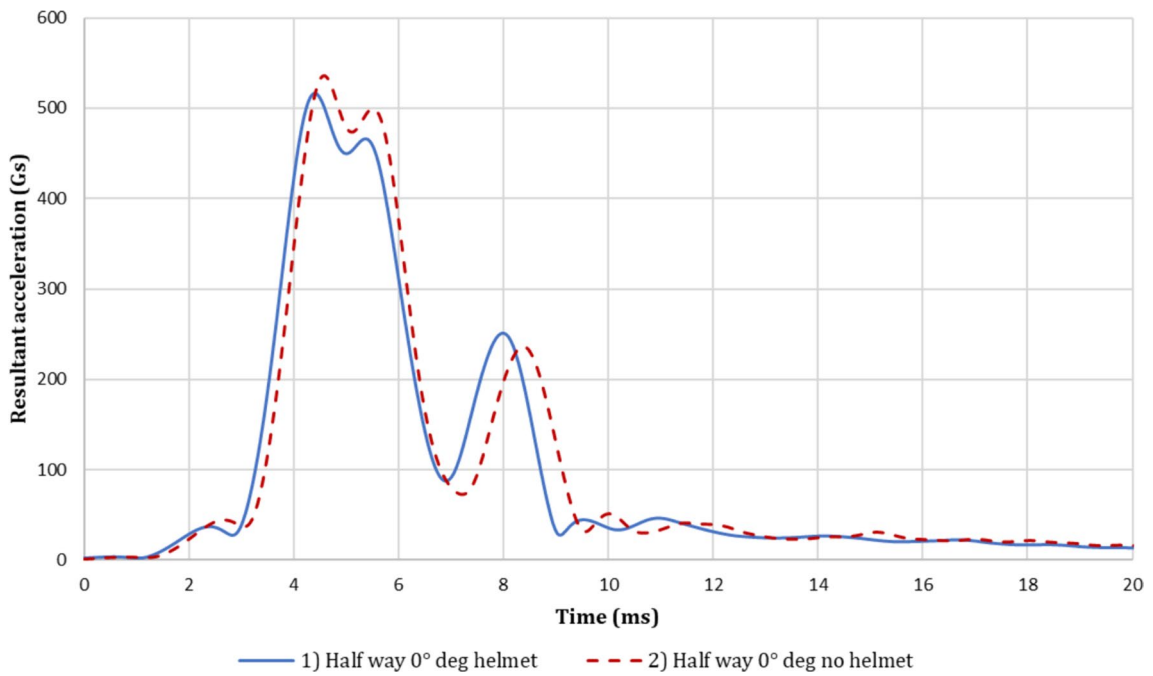


Fig. 8 Resultant acceleration for simulation no.: **a** an impact to the back of the head equipped with a construction hard hat with a construction prop, halfway along the outer prop. HIC: 9 502. **b** An impact to the back of the head with a construction prop halfway down the outer prop. HIC: 10 370

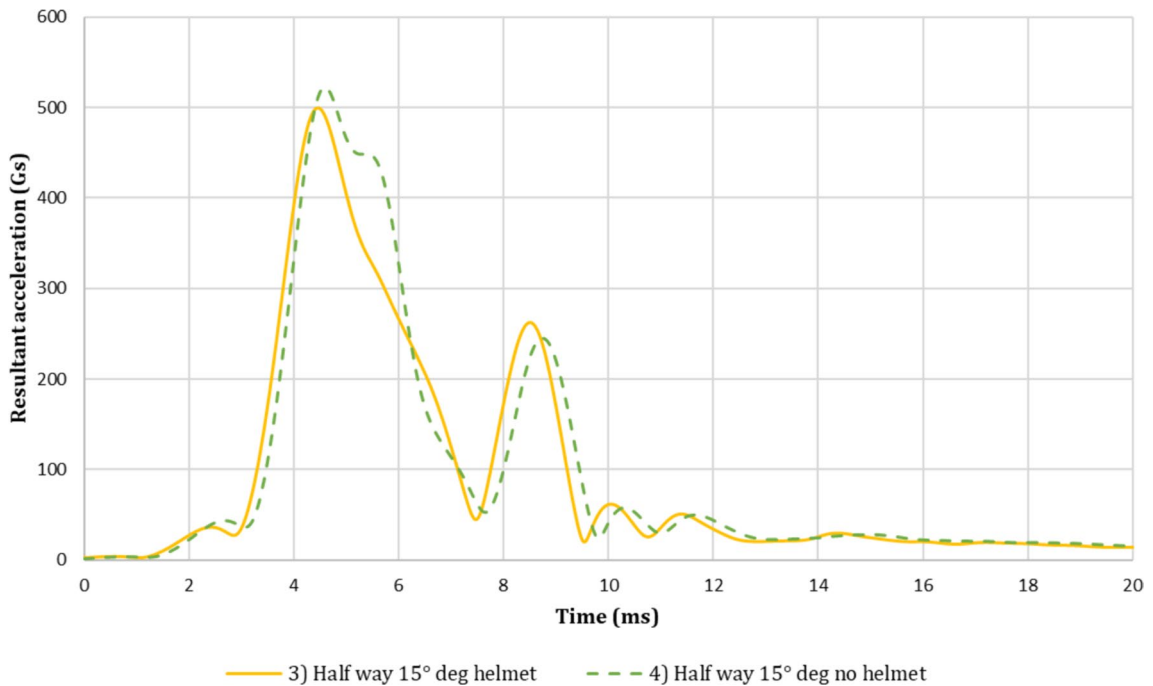


Fig. 9 Resultant acceleration for simulation no.: **c** an impact to the back of the head equipped with a construction hard hat with a construction prop rotated 15° halfway along the outer prop. HIC: 7 810. **d** An impact to the back of the head with a construction prop rotated 15° halfway along the outer prop. HIC: 8 774

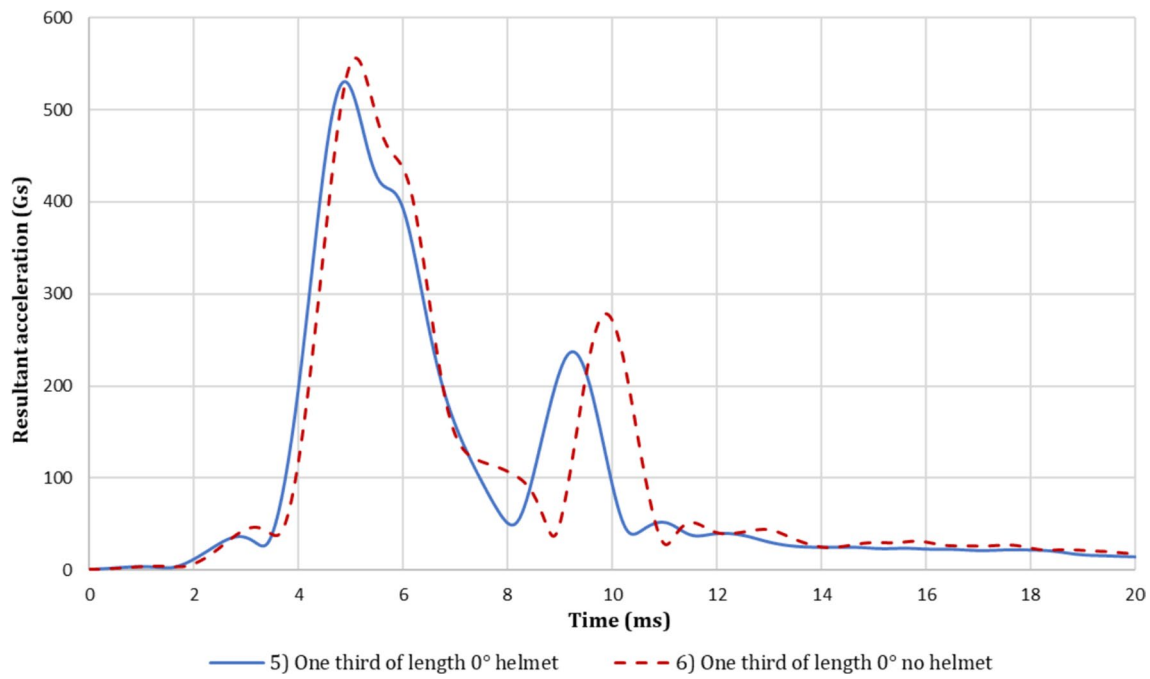


Fig. 10 Resultant acceleration for simulation no.: **e** an impact to the back of the head equipped with a construction hard hat with a construction prop, in one-third of the length of the outer tube, counting from the center of gravity of the entire prop. HIC: 8 354. **f** An impact

to the back of the head with a construction prop, in one-third of the length of the outer prop, counting from the center of gravity of the entire prop. HIC: 9 273

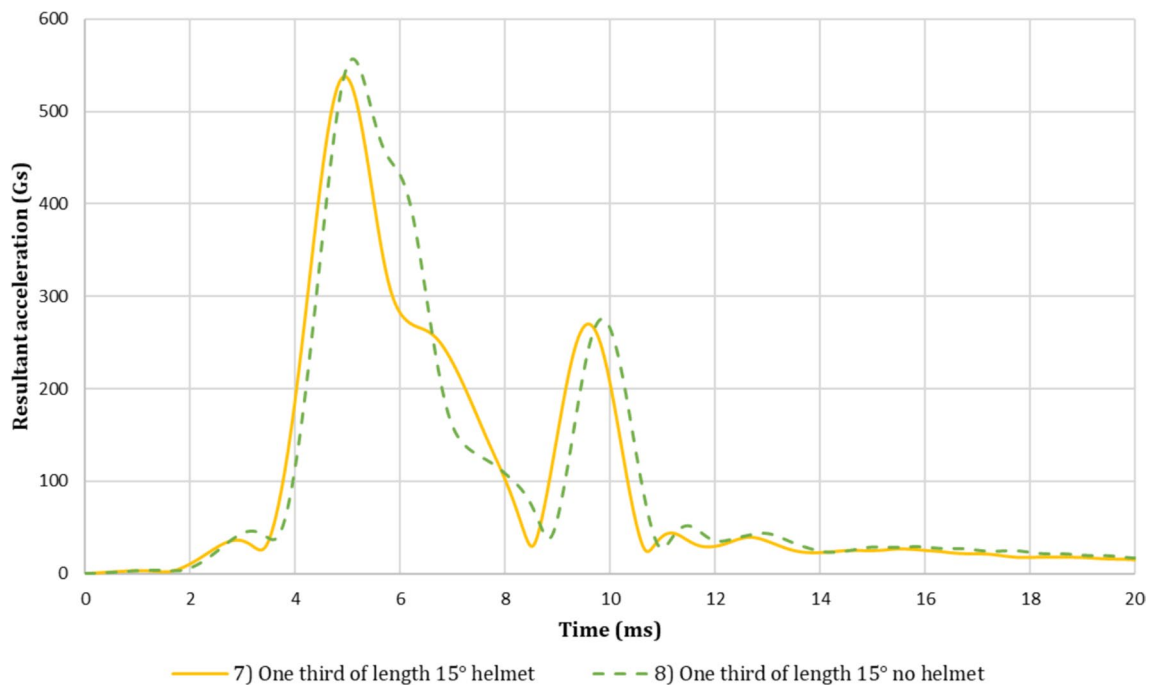


Fig. 11 Resultant acceleration for simulation no.: **g** an impact to the back of the head equipped with a construction hard hat with a construction prop rotated by 15°, in one-third of the length of the outer prop, counting from the center of gravity of the entire prop. HIC: 8

250. **h** An impact to the back of the head with a construction prop rotated by 15°, in one-third of the length of the outer prop, counting from the center of gravity of the entire prop. HIC: 9 229

Funding This research was co-funded by District Court in Krotoszyn, Poland. Moreover, we would like to thank D. Pietrusiak, PhD from Wrocław University of Science and Technology for assisting us with the modal analysis of the helmet.

Declarations

Conflict of interest The authors declare no conflict of interest.

Ethical approval Ethics approval was not required for this research. We obtained consent from the District Court in Krotoszyn, Poland to use the anonymized data for research purposes (dated November 29, 2023).

Open Access This article is licensed under a Creative Commons Attribution 4.0 International License, which permits use, sharing, adaptation, distribution and reproduction in any medium or format, as long as you give appropriate credit to the original author(s) and the source, provide a link to the Creative Commons licence, and indicate if changes were made. The images or other third party material in this article are included in the article's Creative Commons licence, unless indicated otherwise in a credit line to the material. If material is not included in the article's Creative Commons licence and your intended use is not permitted by statutory regulation or exceeds the permitted use, you will need to obtain permission directly from the copyright holder. To view a copy of this licence, visit <http://creativecommons.org/licenses/by/4.0/>.

References

- Takala J. Global estimates of fatal occupational accidents. *Epidemiology*. 1999;10:640–6.
- Commissione europea.; Comunità europea. Istituto statistico. Europäische Sozialstatistik: Arbeitsunfälle Und Arbeitsbedingte Gesundheitsbeschwerden : Daten 1994–2000; Office des publications officielles des Communautés européennes, 2002; ISBN 9289436018.
- Personick M. Serious injuries befall workers struck by objects. *Saf Health*. 1998;1998:68–72.
- Aneziris ON, Papazoglou IA, Mud M, Damen M, Bellamy LJ, Manuel HJ, Oh J. Occupational risk quantification owing to falling objects. *Saf Sci*. 2014;69:57–70. <https://doi.org/10.1016/j.ssci.2014.02.017>.
- Nill RJ. How to select and use personal protective equipment. In: *Handbook of occupational safety and health*. Wiley; 2019. p. 469–94.
- Sone JY, Kondziolka D, Huang JH, Samadani U. Helmet efficacy against concussion and traumatic brain injury: a review. *J Neurosurg*. 2017;126(3):768–81.
- Gilchrist A, Mills NJ. Construction site workers helmets. *J Occup Accid*. 1987;9:199–211. [https://doi.org/10.1016/0376-6349\(87\)90012-5](https://doi.org/10.1016/0376-6349(87)90012-5).
- Long J, Yang J, Lei Z, Liang D. Simulation-based assessment for construction helmets. *Comput Methods Biomech Biomed Eng*. 2015;18:24–37. <https://doi.org/10.1080/10255842.2013.774382>.
- Murali B, Nagarani J. Design and fabrication of construction helmet by using hybrid composite material. In: *Proceedings of the 2013 International conference on energy efficient technologies for sustainability*. IEEE; 2013. p. 145–7.
- Fernandes FAO, Alves de Sousa RJ. Motorcycle helmets—a state of the art review. *Accid Anal Prev*. 2013;56:1–21. <https://doi.org/10.1016/j.aap.2013.03.011>.
- Fernandes FAO, de Sousa RJA, Ptak M, Migueis G. Helmet design based on the optimization of biocomposite energy-absorbing liners under multi-impact loading. *Appl Sci*. 2019. <https://doi.org/10.3390/app9040735>.
- Karliński J, Ptak M, Dziafak P, Rusiński E. The approach to mining safety improvement: accident analysis of an underground machine operator. *Arch Civil Mech Eng*. 2016;16:503–12. <https://doi.org/10.1016/j.acme.2016.02.010>.
- Jacob A, Faria C, Cardoso G, Reis K, Motta M, Meneghetti T, Cammino R, Shibli A. Evaluation of helmet protection during impact of head to ground and impact of an object to head using finite element analysis. *J Saf Eng*. 2015;5:8–16. <https://doi.org/10.5923/j.safety.20160501.02>.
- Wu JZ, Pan CS, Wimer BM, Rosen CL. Finite element simulations of the head-brain responses to the top impacts of a construction helmet: effects of the neck and body mass. *Proc Inst Mech Eng H*. 2017;231:58–68. <https://doi.org/10.1177/0954411916678017>.
- Wdowicz D, Ptak M. Numerical approaches to pedestrian impact simulation with human body models: a review. *Arch Comput Methods Eng*. 2023;30:4687–709.
- Olson BD, Smith CC. A modular dynamic simulation approach to the reconstruction of automobile accidents. *J Dyn Syst Meas Control*. 1983;105:279–86. <https://doi.org/10.1115/1.3140671>.
- Shen J, Jin X-L. Improvement in numerical reconstruction for vehicle—pedestrian accidents proceedings of the institution of mechanical engineers, part D. *J Automob Eng*. 2008;222:25–39. <https://doi.org/10.1243/09544070JAUTO660>.
- Portal RJF, Dias JMP. Multibody models for vehicle accident reconstruction. In: *III european conference on computational mechanics*. Netherlands: Springer; 2008. p. 775–775.
- Moser A, Steffan H, Kasanický G. The pedestrian model in PC-crash - the introduction of a multi body system and its validation. *SAE Technical Paper* 1999-01-0445; 1999. <https://doi.org/10.4271/1999-01-0445>.
- Krašna S, Prebil I, Hribernik M. Human body modelling for traffic accident analysis. *Veh Syst Dyn*. 2007;45:969–80. <https://doi.org/10.1080/00423110701538296>.
- Wach W, Unarski J. Fall from height in a stairwell—mechanics and simulation analysis. *Forensic Sci Int*. 2014;244:136–51. <https://doi.org/10.1016/j.forsciint.2014.08.018>.
- Dejneka A, Małachowski J, Mazurkiewicz Ł. Identification of muscle movements and activity by experimental methods for selected cases—stage #2. *Acta Bioeng Biomech*. 2022. <https://doi.org/10.37190/ABB-02104-2022-02>.
- Deng G, Wang F, Yu C, Peng Y, Xu H, Li Z, Hou L, Wang Z. Assessment of standing passenger traumatic brain injury caused by ground impact in subway collisions. *Accid Anal Prev*. 2022;166:106547. <https://doi.org/10.1016/j.aap.2021.106547>.
- Liu Y, Wan X, Xu W, Shi L, Deng G, Bai Z. An intelligent method for accident reconstruction involving car and e-bike coupling automatic simulation and multi-objective optimizations. *Accid Anal Prev*. 2022;164:106476. <https://doi.org/10.1016/j.aap.2021.106476>.
- Yao J, Yang J, Otte D. Investigation of head injuries by reconstructions of real-world vehicle-versus-adult-pedestrian accidents. *Saf Sci*. 2008;46:1103–14. <https://doi.org/10.1016/j.ssci.2007.06.021>.
- Weng Y, Jin X, Zhao Z, Zhang X. Car-to-Pedestrian Collision Reconstruction with Injury as an Evaluation Index. *Accid Anal Prev*. 2010;42:1320–5. <https://doi.org/10.1016/j.aap.2010.02.012>.
- Ptak M. Pedestrian safety: a new method to assess pedestrian kinematics. *Transport*. 2018;33:41–51. <https://doi.org/10.3846/transport.2019.7081>.
- Guzek M, Lozia Z. Computing Methods in the Analysis of Road Accident Reconstruction Uncertainty. *Arch Comput Methods Eng*. 2021;28:2459–76. <https://doi.org/10.1007/s11831-020-09462-w>.
- Wach, W.; Unarski, J. Uncertainty analysis of the preimpact phase of a pedestrian collision. in *proceedings of the SAE Technical Paper* 2007–01–0715; April 16 2007.

30. Rawska K, Gepner B, Kerrigan JR. Effect of various restraint configurations on submarining occurrence across varied seat configurations in autonomous driving system environment. *Traffic Inj Prev.* 2021;22:S128–33. <https://doi.org/10.1080/15389588.2021.1939872>.
31. Srinivas V, Sasmal S, Ramanjaneyulu K, Jeyasehar CA. Influence of test conditions on modal characteristics of reinforced concrete structures under different damage scenarios. *Arch Civil Mech Eng.* 2013. <https://doi.org/10.1016/j.acme.2013.04.006>.
32. Odyjas P, Więckowski J, Pietrusiak D, Moczko P. Challenges in the Design of a New Centrifugal Fan with Variable Impeller Geometry. *Acta Mechanica et Automatica.* 2023. <https://doi.org/10.2478/ama-2023-0002>.
33. Sybilski K, Mazurkiewicz Ł, Jurkojć J, Michnik R, Małachowski J. Evaluation of the effect of muscle forces implementation on the behavior of a dummy during a head-on collision. *Acta Bioeng Biomech.* 2021. <https://doi.org/10.37190/ABB-01976-2021-04>.
34. Baghaei SM, Sadegh AM, Charles S. Characteristics of HIC in prediction of MTBI relating to crash pulses. *Int J Veh Des.* 2019;80:59. <https://doi.org/10.1504/IJVD.2019.105066>.
35. Marjoux D, Baumgartner D, Deck C, Willinger R. Head injury prediction capability of the HIC, HIP, SIMon and ULP criteria. *Accid Anal Prev.* 2008;40:1135–48. <https://doi.org/10.1016/j.aap.2007.12.006>.
36. Dymek M, Ptak M, Ratajczak M, Fernandes FAO, Kwiatkowski A, Wilhelm J. Analysis of HIC and hydrostatic pressure in the human head during NOCSAE tests of American football helmets. *Brain Sci.* 2021;11:287. <https://doi.org/10.3390/brainsci11030287>.
37. Špička J, Boňkowski T, Hynčík L, Hanuliak A. Assessment of nanobag as a new safety system in the frontal sled test. *Appl Sci.* 2022. <https://doi.org/10.3390/app12030989>.
38. Yu H, Sun Y, Jia C. Safety helmet wearing detection based on super-resolution reconstruction. In: *Proceedings of the IEEE information technology, networking, electronic and automation control conference, ITNEC.* IEEE; 2021.
39. Pan CS, Wimer BM, Welcome DE, Wu JZ. An approach to characterize the impact absorption performance of construction helmets in top impact. *J Test Eval.* 2022. <https://doi.org/10.1520/JTE20180604>.
40. Human Factors in Protective Headgear Design. In *Human Factors and Ergonomics in Consumer Product Design: Uses and Applications*; 2011.
41. Bottlang M, DiGiacomo G, Tsai S, Madey S. Effect of helmet design on impact performance of industrial safety helmets. *Heliyon.* 2022. <https://doi.org/10.1016/j.heliyon.2022.e09962>.
42. Kung SM, Suksreephaisan TK, Perry BG, Palmer BR, Page RA. The effects of anticipation and visual and sensory performance on concussion risk in sport: a review. *Sports Med Open.* 2020. <https://doi.org/10.1186/s40798-020-00283-6>.
43. MacManus DB, Ghajari M. Material properties of human brain tissue suitable for modelling traumatic brain injury. *Brain Multiphys.* 2022;3:100059. <https://doi.org/10.1016/j.brain.2022.100059>.

Publisher's Note Springer Nature remains neutral with regard to jurisdictional claims in published maps and institutional affiliations.